Physica E 121 (2020) 114149

Contents lists available at ScienceDirect

Physica E: Low-dimensional Systems and Nanostructures

journal homepage: www.elsevier.com/locate/physe

Effects of charged impurity scattering and substrate on the magneto-optical absorption properties in gapped monolayer graphene

Pham T. Huong [a,b], Le T. Hoa [c,d], Van Thinh Pham [e], Hoang D. Long [f], Nguyen N. Hieu [c,d], Huynh V. Phuc [g], Chuong V. Nguyen [h], Bui D. Hoi [i,*]

[a] Division of Computational Mathematics and Engineering, Institute for Computational Science, Ton Duc Thang University, Ho Chi Minh City, Viet Nam
[b] Faculty of Environment and Labour Safety, Ton Duc Thang University, Ho Chi Minh City, Viet Nam
[c] Institute of Research and Development, Duy Tan University, Da Nang 550000, Viet Nam
[d] Faculty of Natural Sciences, Duy Tan University, Da Nang 550000, Viet Nam
[e] Center of Excellence for Green Energy and Environmental Nanomaterials, Nguyen Tat Thanh University, Ho Chi Minh City, Viet Nam
[f] Department of Physics, University of Education, Hue University, Hue, Viet Nam
[g] Division of Theoretical Physics, Dong Thap University, Cao Lanh, Viet Nam
[h] Department of Materials Science and Engineering, Le Quy Don Technical University, Hanoi, Viet Nam
[i] Center for Theoretical and Computational Physics and Department of Physics, University of Education, Hue University, Hue, Viet Nam

ABSTRACT

Motivated by some earlier experimental observations on the magneto-optical absorption and cyclotron resonance in graphene, we carry out systematically a theoretical investigation of the magneto-optical absorption in graphene monolayer situated on a substrate. The effect of electron-impurity scattering is considered at low temperatures. The magneto-optical absorption coefficient (AC) is calculated using the perturbation theory taking account of both one- and two-photon absorption processes. Numerical results are obtained for the SiO_2, SiC, and h-BN substrates to compare and show effects of the substrate. There appear the cyclotron-impurity resonance peaks in the AC which show a blue-shift with increasing magnetic field strength. In general, the absorption intensity, the resonance energy and the FWHM depend strongly on the substrate. Also, the FWHM increases with increasing the impurity density by the law FWHM= $\beta\sqrt{n_i}$, where β is a constant whose value is different in different substrates and n_i the impurity density. In particular, the resonance energy versus magnetic field strength and the full width at half maximum (FWHM) for the SiO_2 substrate are in good agreement with those obtained by earlier experiments.

1. Introduction

Since its successful fabrication, graphene has become one of the most attractive materials in condensed matter physics and materials science. It is also a motivation to study and fabricate many other graphene-like materials. Studies related to graphene have exploded rapidly, both fundamentally and in applications [1–4]. One of the physical properties of graphene, that is of great interest, is the magneto-optical transport property, motivated by its potential applications. Cyclotron resonance (CR) in graphene has been studied both theoretically [5] and experimentally [6,7]. The phonon-assisted CR in graphene monolayers have also been studied at high temperatures when the electron–phonon interaction is considered as the main perturbation causing electron transition in the case of free standing graphene [8] and the graphene layer on a polar substrate [9]. In the work [5], the magneto-optical conductivity in single-layer graphene was theoretically calculated using the Kubo–Mori formula. The authors analysed in detail the resonance conditions with possible transitions of charged carriers. However, they only considered the linear (one-photon) absorption of the optical field and did not include any effect of carrier scattering. On the other hand, many studies have shown that transport properties in solids cannot be well explained by considering carriers being scattered only by the lattice (phonon), in particular at low temperatures [10]. At low temperatures, impurity scattering is superior to lattice (phonon) scattering and should be taken into account in investigating quantum effects which are pronounced at such temperatures. The electron-impurity scattering in graphene has been included in investigating the quantum Hall effect [11], the density of states and magneto-optical conductivity in a perpendicular magnetic field [5], the Landau broadening in strong magnetic fields [12], and the magnetotransport in a dc bias current where the Shubnikov–de Haas oscillation in the magnetoresistivity was examined [13]. It can be believed that the electron-impurity scattering has a significant effect on the magneto-optical absorption properties in graphene because it modifies the electron density of states and electron transition probability between electronic states.

On the other hand, graphene monolayer has zero band gap and so cannot be applied in on–off devices. To possibly apply graphene in such devices, it is necessary to turn graphene into a semiconductor,

* Corresponding author.
E-mail addresses: phamthihuong@tdtu.edu.vn (P.T. Huong), lethihoa8@duytan.edu.vn (L.T. Hoa), buidinhhoi@hueuni.edu.vn (B.D. Hoi).

https://doi.org/10.1016/j.physe.2020.114149
Received 10 March 2020; Received in revised form 18 April 2020; Accepted 20 April 2020
Available online 23 April 2020

i.e., create a large enough band gap in graphene. There have been some ways to open a band gap in graphene. One of them is placing the graphene monolayer on a polar substrate. By interacting with the substrate, two sublattices of graphene become inequivalent. This means that the sublattice symmetry is directly broken and a mass term in the Dirac Hamiltonian of fermions is generated, i.e., a band gap is opened. The band gap in graphene monolayer has been reported to be about 106 meV and 260 meV for h-BN [14–16] and SiC substrate [17,18], respectively. Even, the Cu(100) substrate exposed to the air can induce a larger band gap of 350 meV in graphene layer. The small value of the band gap results in the change in the carrier energy dispersion, hence is predicted to cause the shifting of optical absorption peaks arising from the selection rules, in comparison with the gapless case. Therefore, it should not be neglected in theoretical considerations.

In this work, we investigate theoretically the magneto-optical absorption in a graphene monolayer placed on a substrate and subjected to a perpendicular static magnetic field. The magneto-optical absorption coefficient (AC) is derived by using perturbation theory and numerically calculated for different substrates. Our work has some new features in comparison with earlier theoretical works [5,8,9] because we consider simultaneously: (1) the effect of electron-impurity scattering at low temperatures, (2) a small band gap induced by the polar substrate in the electronic band structure of monolayer graphene, (3) the two-photon absorption beside the usual one-photon absorption. The paper is structured as follows. In Section 2, we introduce the electronic band structure and the total electron-impurity interacting Hamiltonian in gapped graphene. Section 3 presents briefly the derivation of the magneto-optical absorption coefficient (AC). Numerical results and discussion are presented in Section 4. Finally, remarkable conclusions are listed in Section 5.

2. Electronic band structure in gapped graphene and Hamiltonian of electron-impurity system

In this investigation, we consider a model of graphene sheet grown on a polar substrate. The polar substrate is assumed to break the symmetry of two carbon sublattices (named A and B) in the graphene layer and induces a finite band gap in its electronic band structure. Applying a uniform static magnetic field ($\vec{B}$) perpendicularly to the graphene sheet and choosing the vector potential in the Landau gauge simply to be $\vec{A} = (-By, 0)$, the unperturbed (non-interacting) Hamiltonian for Dirac fermions in the vicinity of the K point, has the form [11]

$$H_0 = \begin{pmatrix} \Delta & v_F\pi_- \\ v_F\pi_+ & -\Delta \end{pmatrix}, \tag{1}$$

with $\pi_\pm = p_x \pm \mathrm{i}p_y - eBy$ being the momentum operators, v_F the Fermi velocity and 2Δ being the opened band gap, i.e., the on-site energy difference between the carbon atoms A and B or the distance between the conduction band minimum and the valence band maximum. Here, we have neglected the small spin–orbit coupling in graphene. Also, the Zeeman splitting effect is not included in this investigation because it is considerable at very strong magnetic fields only ($B > 20$ T) [19,20].

The normalized eigenvectors of H_0 have been introduced in [11] and are given by

$$\Psi_n = \frac{1}{\sqrt{L_x}} \begin{pmatrix} a_{ns}\phi_{n-1} \\ s b_{ns}\phi_n \end{pmatrix} e^{\mathrm{i}k_x x}, \tag{2}$$

where $\phi_n(Y)$ are the usual oscillator functions with $Y = (y - \ell_c^2 k_x)/\ell_c$, $\ell_c = \sqrt{\hbar/eB}$ is the magnetic length or the radius of Landau orbit. n ($n = 1, 2, \ldots$) is the index of the Landau levels, $s = +1$ ($s = -1$) for the conduction (valence) band, and

$$a_{ns} = \sqrt{\frac{E_{n,s} + \Delta}{2E_{n,s}}}, \quad b_{ns} = \sqrt{\frac{E_{n,s} - \Delta}{2E_{n,s}}} \tag{3}$$

with $E_{n,s}$ being the eigenvalues of the Hamiltonian (1). Furthermore, as shown previously [11], the level $n = 0$ must be treated separately and one can obtain its normalized eigenvector as

$$\Psi_0 = \frac{1}{\sqrt{L_x}} \begin{pmatrix} 0 \\ \phi_0 \end{pmatrix} e^{\mathrm{i}k_x x}. \tag{4}$$

The eigenvalues, $E_{n,s}$, are given for $0 \le n$ by [11]

$$E_{n,s} = s\left[\Delta^2 + n\hbar^2\omega_c^2\right]^{1/2}(1 - \delta_{n0}), \quad E_{0,s} = \mp\Delta\delta_{n0}, \tag{5}$$

where $\omega_c = \sqrt{2}v_F/\ell_c = (v_F\sqrt{2e/\hbar})\sqrt{B}$ with v_F being the Fermi velocity. The sign of the zeroth level energy E_{0s} is negative for the K point and positive for the K' point. It is believed that the magneto-optical transport takes place equivalently at the K and K' points, so in the following we consider only the K point as an example.

We now assume that carriers in the graphene sheet are mainly scattered by charged impurities in the substrate at low temperatures. Then the Hamiltonian of the electron-impurity system has the form

$$H = H_0 + H_{e-i}, \tag{6}$$

where H_{e-i} is the electron-impurity interacting Hamiltonian and is given in the Landau representation as [13,21]

$$H_{e\text{-}i} = \sum_{\vec{q},a}\sum_{\xi,\xi'} U(q)F_{\xi\xi'}(q)e^{\mathrm{i}\vec{q}(\vec{R}-\vec{r}_a)}c_\xi^+ c_{\xi'}, \tag{7}$$

where we have defined $\Psi_n \equiv |\xi\rangle = |n, s, k_x\rangle$, $\vec{q}$ is the change in the electron wave vector, $\vec{R}$ and $\vec{r}_a$ are the positions of a carrier and an impurity, respectively, $U(q)$ is the Fourier transform of the scattering potential between carrier and charged impurities, c_ξ^+ (c_ξ) is the creation (annihilation) operator of electron in the state $|\xi\rangle$. The sum is over all quantum numbers n, s, k_x and $\vec{q}, a$. In this calculation, we also assume that charged impurities are situated in a 2D plane in the substrate and have the same distance d from the graphene sheet. The scattering potential, taking account of the $e - e$ screening effect, is then given by [12]

$$U(q) = \frac{Ze^2}{2\epsilon_0\kappa_i(q + q_s)}\mathrm{e}^{-qd}, \tag{8}$$

where ϵ_0 is the vacuum permittivity, κ_i is the dielectric constant for impurities in the substrate with Z being the impurity charge number, q_s is the inverse screening wave length which can be obtained within the random-phase approximation [5,11], and $F_{\xi\xi'}(q) = \langle\xi|e^{\mathrm{i}qr_a}|\xi'\rangle$ is the form factor for electron-impurity scattering which has been evaluated analytically to be [5,11]

$$|F_{\xi\xi'}(q)|^2 = \frac{m!}{(m+j)!}e^{-u}u^j \times \left[a_{ns}a_{n's'}\sqrt{\frac{m+j}{m}}L_{m-1}^j(u) + b_{ns}b_{n's'}L_m^j(u)\right]^2. \tag{9}$$

Here, $m = \min(|n|, |n'|)$, $j = \left||n'| - |n|\right|$, and $L_m^j(u)$ being the associated Laguerre polynomials with $u = \ell_c^2 q^2/2$.

3. Expression for the nonlinear absorption coefficient

We now consider the optical absorption in the above graphene sheet when it is further stimulated by an electromagnetic wave (optical field) of the frequency ω and electric field amplitude E_0. We assume the same kind of impurities which are randomly distributed in the 2D plane of the substrate. Therefore, the carrier-impurity scattering strength is the same for all charged impurities and the position of each impurity can be regardless. The transition probability of electrons between the states $|\xi\rangle$ and $|\xi'\rangle$ due to carrier-impurity-photon scattering for the ℓ-photon process can be given by [22]

$$W_{\xi,\xi'}^{\ell} = \frac{2\pi n_i}{\hbar S_0}\sum_q\sum_{\ell=1}^{\infty}|U(q)|^2|F_{\xi\xi'}(q)|^2\ell J_\ell^2(\alpha_0 q)$$

Table 1
Some parameters used in the present numerical calculations.

Substrate	2Δ (meV)	κ_i	d (Å)
SiO_2	0 [29]	4.25 [12]	4 [13]
SiC	260 [30]	9 [31]	2 [18]
h-BN	53 [14,32]	3 [14,32]	3.22 [14,32]

$$\times\ \delta_{k_x,k'_x+q_x}\delta(E_{n's'}-E_{ns}-\ell\hbar\omega), \tag{10}$$

where n_i is the impurity density, S_0 the area of the sample, α_0 is the dressing parameter, $J_\ell(x)$ is the Bessel function of the argument x. The AC by electrons is related to the transition probability by [22]

$$\Gamma = \frac{16\pi\hbar n_0}{c\sqrt{\epsilon_\infty}a_0^2\omega}\left[1-e^{-\hbar\omega/(k_BT)}\right]\sum_{\xi,\xi'} f(E_\xi)(1-f(E_{\xi'}))W^\ell_{\xi,\xi'}, \tag{11}$$

where $f(E_\xi)$ is the equilibrium Fermi–Dirac distribution for electron, n_0 is the electrons density, $a_0 = E_0/\omega$, c is the speed of light in free space, k_B is the Boltzmann constant, T the absolute temperature, and $\epsilon(\omega)$ is the high-frequency dielectric constant in graphene. It should be noted that in Eq. (11) the sum is over all quantum numbers $|\xi\rangle = |n, s, k_x\rangle$ and $|\xi'\rangle = |n', s', k'_x\rangle$ with $|\xi\rangle \neq |\xi'\rangle$.

It has been shown that the two-photon absorption contributes considerably to the total absorption beside the crucial one-photon absorption [23–28]. Therefore, in the following we will take account of both the one-photon ($\ell = 1$) and two-photon ($\ell = 2$) absorption in the expression of the AC. To obtain an explicit expression for the AC, one needs the following transformations [11] $\sum_q \to \frac{S_0}{(2\pi\ell_c)^2}\int_0^\infty du\int_0^{2\pi} d\varphi$, and $\sum_{\xi/\xi'} \to \frac{g_s S_0}{2\pi\ell_c^2}\sum_{n,s/n',s'}$, where $g_s = 2$ is the spin degeneracy. After a straightforward calculation, we have the expression for AC

$$\begin{aligned}\Gamma &= \frac{4n_0n_iS_0^2e^4Z^2}{c\sqrt{\epsilon_\infty}\pi a_0^2\omega\ell_c^6\epsilon_0^2\kappa_i^2q_s^2}\left[1-e^{-\hbar\omega/(k_BT)}\right]\\ &\times\sum_{nn'ss'} f(E_{ns})\left[1-f(E_{n's'})\right]\left\{\frac{\alpha_0^2}{2\ell_c^2}H^{(1)}_{nn'ss'}\delta(E_{n's'}-E_{ns}-\hbar\omega)\right.\\ &\left.+\frac{\alpha_0^4}{8\ell_c^4}H^{(2)}_{nn'ss'}\delta(E_{n's'}-E_{ns}-2\hbar\omega)\right\},\end{aligned} \tag{12}$$

where

$$H^{(p)}_{nn'ss'} = \int_0^\infty u^p e^{-2d\sqrt{2u}/\ell_c}|F_{\xi\xi'}(u)|^2du, \tag{13}$$

with $p = 1, 2$ and will be computationally evaluated in the next section. As usual, the divergence of the delta functions in (12) can be avoided by approximately replacing them by the Lorentzians of the width $\gamma_{n,n'}$ due to scattering by charged impurities given as [5,12]

$$\begin{aligned}\gamma^2_{nn'ss'} &= \sum_q n_i\left(\frac{Ze^2}{2\epsilon_0\kappa_i(q+q_s)}e^{-qd}\right)^2|F_{\xi\xi'}(q)|^2\\ &= n_i\frac{e^4Z^2S_0}{8\pi\ell_c^2\epsilon_0^2\kappa_i^2q_s^2}H^{(0)}_{nn'ss'},\end{aligned} \tag{14}$$

where $H^{(0)}_{nn'ss'}$ is defined in Eq. (13) with $p = 0$. Numerical analyses of the physical behaviours of the AC will be performed and presented in the next section.

4. Numerical results and discussion

To clarify the behaviours of the AC, we now proceed to numerically calculate the AC obtained in Eq. (12). Also, to show the effects of the substrate, we consider the graphene sheet on three typical substrates, SiO_2, SiC, and h-BN. The parameters for these substrates are listed in Table 1. We also choose $n_0 = 10^{12}$ cm^{-2} [12], $Z = 1$ [12], $\alpha_0 = 5$ nm [8,9]. Also, only the principal transition $n = 0 \to n' = 1$ is considered so that the results can be compared with those obtained by other experiments and theories with the same transition therein.

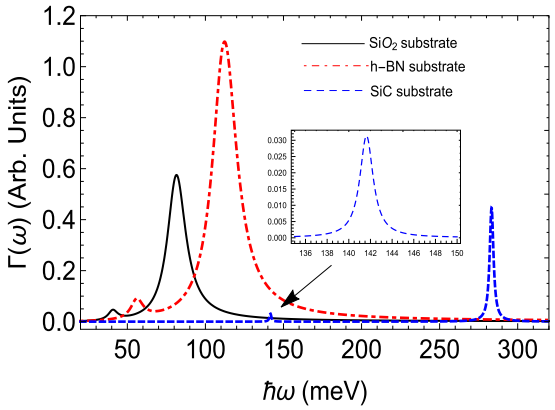

Fig. 1. The AC as a function of photon energy in monolayer graphene on SiO_2, SiC, and h-BN substrates at $B = 5$ T, $n_i = 10^{11}$ cm^{-2}, and $T = 2$ K. The inset is to magnify the peak arising from two-photon absorption for SiC substrate.

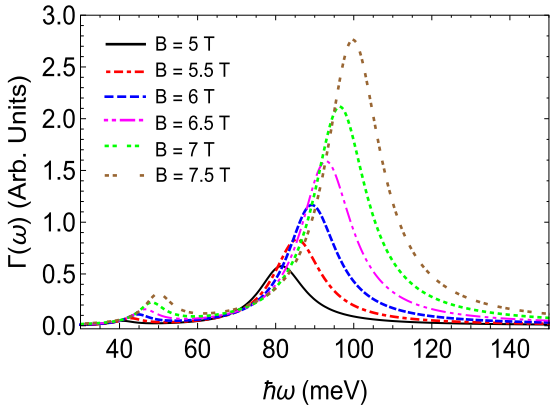

Fig. 2. The AC as a function of photon energy in monolayer graphene on SiO_2 substrate ($\Delta = 0$) at different values of B. Here, $n_i = 10^{11}$ cm^{-2} and $T = 2$ K.

In Fig. 1, the AC is shown as a function of the photon energy for different substrates at the magnetic field strength of 5 T. We can see from the figure the appearance of some maxima in the absorption spectrum. More specifically, each curve has two absorption maxima. One can find that these maxima are the cyclotron-impurity resonant peaks where the electron transitions satisfy the selection rule

$$E_{1,+1} - E_{0,-1} = \ell\hbar\omega, \tag{15}$$

where $\ell = 1$ and 2 for the right and the left peak, respectively. In other words, the right one originates from the one-photon ($\ell = 1$) absorption and the left one from the two-photon ($\ell = 2$) absorption. We also see that for all curves the two-photon absorption peak is always much lower than the one-photon absorption one, for instance, in the case of SiO_2 substrate (gapless graphene) the left peak is only about 9% of the right peak in height. Physically, it implies the fact that the two-photon absorption has a minor contribution but should not be neglected in the total absorption. In addition, it can be seen from Fig. 1 that the AC is largest for the h-BN substrate and smallest for the SiC substrate for both one- and two-photon absorption. For instance, the AC for h-BN substrate is about twice of that for SiC substrate in one-photon absorption case. This shows that the substrate has a strong effect on the absorption intensity.

We now turn to examine how the absorption spectrum changes with the magnetic field variation. In Fig. 2, we show the AC versus the

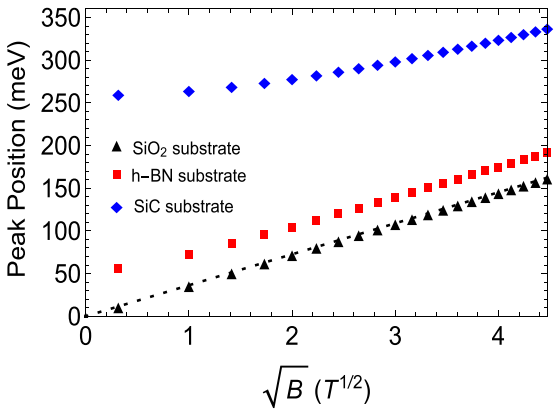

Fig. 3. Peak position (in meV) versus magnetic field for different substrates for one-photon absorption. The dotted straight line is drawn as an orientation for convenient viewing. Here, $n_i = 10^{11}$ cm^{-2} and $T = 2$ K.

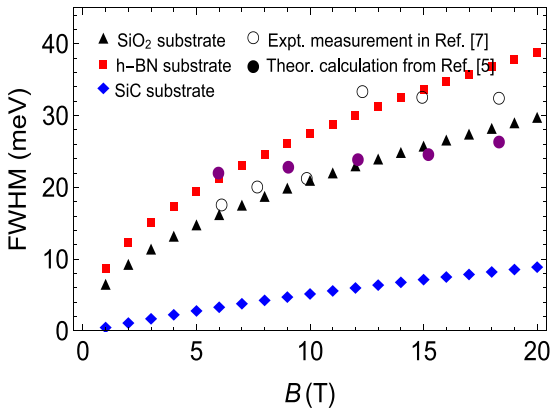

Fig. 4. The FWHM as a function of magnetic field strength for different substrates at $T = 2$ K. The open and filled circles are, respectively, the experiment results in Ref. [7] and theoretical results in Ref. [5].

photon energy for graphene on SiO_2 substrate ($\Delta = 0$) at some different values of magnetic field strength. It is clear from the figure that as the magnetic field strength increases, a blue-shift of the peaks in the AC occurs and the AC value is enhanced. The blue-shift and enhancement in the AC with increasing the magnetic field have been observed before in 2D materials such as graphene [33], silicene [34], and monolayer MoS_2 [35]. In more detail, we compute the relation between the peak position (the resonance energy) and the magnetic field strength for all the substrates as shown in Fig. 3. The blue-shift of the peak position is the consequence of the resonant condition where the resonant photon energy is, in general, equal to the difference of two Landau energy levels, $\hbar\omega = E_{n',s'} - E_{n,s}$, which increases with increasing the magnetic field strength. Also, we can see an interesting thing from Fig. 3 that the resonance energy for the SiO_2 substrate depends linearly on the square root of the magnetic field whereas it shows a nonlinear dependence for the SiC and BN substrates. This can be easily explained by using the resonance condition (15) with the energy spectrum for electrons in gapped graphene in Eq. (7). For SiO_2 substrate, the graphene sheet is gapless ($\Delta = 0$), so the resonance energy $\hbar\omega = E_{1,+1} - E_{0,-1} \propto \hbar\omega_c \propto \sqrt{B}$. However, for SiC and h-BN substrates, because of the non-zero band gap ($\Delta \neq 0$) in the energy spectrum (7) the difference $(E_{1,+1} - E_{0,-1})$ does not depend linearly on $\sqrt{B}$ anymore, and so the resonance energy for these two substrates is not linear with $\sqrt{B}$. Also, it is clear that the larger the band gap Δ, the more nonlinear the relation. The relation between the resonant peak position and magnetic field strength for the SiO_2 substrate obtained here shows a good agreement with previous experimental observations [6,7] and theory [5] (see Fig. 1(c) in Ref. [6] and Fig. 11(a) in Ref. [5]).

The effect of magnetic field on the absorption spectrum can also be shown via investigating the full width at half maximum (FWHM) of the peaks. By computation, we obtain the FWHM and show its dependence on the magnetic field strength in Fig. 4 for all the substrates and one-photon absorption processes. We can see from the figure that the FWHM increases with increasing magnetic field strength for all the substrates. In particular, our calculated FWHMs for SiO_2 substrate case are in good agreement with those obtained experimentally in Refs. [6,7] and by theory in Ref. [5] with the same electron transition and substrate. Also, it can be seen from Fig. 4 that at a fixed magnetic field, the FWHM is largest and smallest for the h-BN and SiC substrate, respectively. For example, at $B = 5$ T the FWHM is 3.06, 14.95, and 19.80 meV, respectively, for the SiC, SiO_2, and h-BN. At this point, however, we cannot deduce a general law for the effect of substrate on the FWHM because the FWHM is mathematically governed by the broadening parameter $\gamma_{n,n'}$ given by Eq. (14) which is determined by substrate's parameters such as the substrate dielectric constant, the

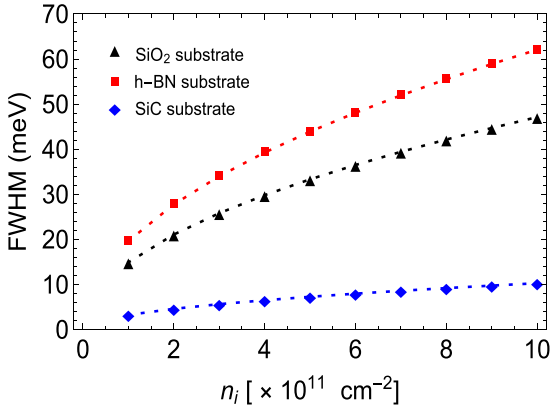

Fig. 5. The FWHM as a function of impurity density for different substrates at $T = 2$ K and $B = 5$ T.

graphene-substrate distance, the impurity density distributed in substrate, the carrier-impurity scattering mechanism, and so on. Further studies on the individual effect of these parameters on the optical absorption should be carried out separately. As mentioned above, we assume the same kind of impurities and the carrier-impurity scattering strength then is constant. Therefore, we now examine only the effect of impurity density on the optical absorption. It should be noted that the position of resonant peaks determined by Eq. (15) is independent of the impurity density and hence, only the impurity density-dependent FWHM is necessary to be investigated. The FWHM is calculated at different values of impurity density and shown in Fig. 5. We can see clearly the increase of the FWHM with impurity density for all the substrates. By using the data fit, one can obtain the law in all the substrates as FWHM [meV] = $\beta\sqrt{n_i}$, where $\beta = 4.712 \times 10^{-3}$, 1.028×10^{-3}, 6.208×10^{-3} meV/m^{-1}, respectively, for the SiO_2, SiC, h-BN substrate and n_i is in the unit of cm^{-2}. This law is consistent with the impurity density dependence of the broadening parameter $\gamma_{n,n'}$ which determines the FWHM of the resonant peaks, namely $\gamma_{n,n'} \sim \sqrt{n_i}$ as introduced in Eq. (14). Physically, the FWHM is proportional to the electron transition probability which is enhanced as the impurity density increases.

Having examined the effects of magnetic field and impurity density on the absorption properties, we now consider further the effect of the temperature on the FWHM. The dependence of the FWHM on the temperature is shown in Fig. 6 at the magnetic field of 1 T. It is

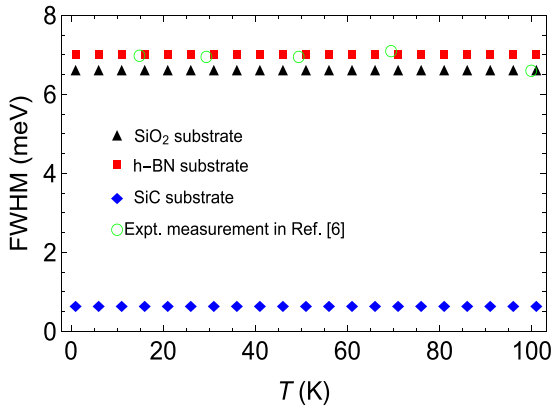

Fig. 6. Dependence of the FWHM on temperature for different substrates at $B = 1$ T. The open circles are the experimental data taken from Ref. [6]. Here, $n_i = 10^{11}$ cm^{-2}.

clear that the FWHM does not vary with temperature as expected. Our result is in good agreement with the experimental results reported in Ref. [6] for the same temperature range and magnetic field strength (see Fig. 3(b) therein). Moreover, the stability of the FWHM with temperature proves that the approximation of the delta functions by the Lorentzians with the broadening parameter $\gamma_{n,n'}$ in Eq. (14) is reasonable in this investigation.

5. Conclusions

In summary, we have theoretically investigated the magneto-optical absorption in gapped monolayer graphene on a substrate. The AC and FWHM have been calculated and numerically analysed for SiO_2, SiC, and h-BN substrates. In general, the AC for two-photon absorption processes is much smaller than it is for one-photon absorption but plays an important role in nonlinear optics. The magnetic field-dependent and temperature-dependent FWHMs are in good agreement with previous experimental and theoretical results. The FWHM increases with increasing the impurity density by the law FWHM $= \beta\sqrt{n_i}$ where β is a constant getting different values for different substrates. Besides, the effects of the substrate on the magneto-optical absorption in the graphene layer can be summarized as follows. First, the finite induced band gap in graphene by the substrate leads to a nonlinear dependence of the resonance energy on the square root of magnetic field strength, that is different from the gapless case. Also, the larger the band gap induced, the more evident the nonlinearity. Second, both the absorption intensities and FWHMs are considerably different in different substrates. The AC and FWHM are largest for the h-BN substrate and smallest for the SiC substrate. However, we cannot specify which parameter of the substrate determines the value of these quantities. The substrate dependence of the absorption intensity as well as the FWHM in monolayer graphene suggests a possibility of controlling the absorption properties by using an appropriate substrate.

Declaration of competing interest

The authors declare that they have no known competing financial interests or personal relationships that could have appeared to influence the work reported in this paper.

CRediT authorship contribution statement

Pham T. Huong: Conceptualization, Investigation, Formal analysis, Writing - review & editing. **Le T. Hoa:** Conceptualization, Investigation, Formal analysis. **Van Thinh Pham:** Conceptualization, Software, Formal analysis, Writing - review & editing. **Hoang D. Long:** Conceptualization, Software, Formal analysis, Writing - review & editing. **Nguyen N. Hieu:** Conceptualization, Software, Formal analysis, Writing - review & editing. **Huynh V. Phuc:** Conceptualization, Software, Formal analysis, Writing - review & editing. **Chuong V. Nguyen:** Conceptualization, Software, Formal analysis, Writing - review & editing. **Bui D. Hoi:** Conceptualization, Methodology, Investigation, Formal analysis, Writing - review & editing.

Acknowledgement

B. D. H. would like to acknowledge the support by Hue University within the Grant No. DHH2018-03-114.

References

[1] S. Sahoo, G.C. Nayak, Present status and prospect of graphene research, in: S. Sahoo, S. Tiwari, G. Nayak (Eds.), Surface Engineering of Graphene, in: Carbon Nanostructures, Springer, Cham, 2019.
[2] Maria Coroș, Florina Pogăcean, Lidia Măgeruşan, Crina Socaci, Stela Pruneanu, Front. Mater. Sci. 13 (2019) 23.
[3] H. Cheun Lee, et al., RSC Adv. 7 (2017) 15644.
[4] Yanxia Wu, Shengxi Wang, Kyriakos Komvopoulos, J. Mater. Res. 35 (1) (2020) 76.
[5] C.H. Yang, F.M. Peeters, W. Xu, Phys. Rev. B 82 (2010) 205428.
[6] M. Orlita, et al., Phys. Rev. Lett. 101 (2008) 267601.
[7] Z. Jiang, E.A. Henriksen, L.C. Tung, Y.-J. Wang, M.E. Schwartz, M.Y. Han, P. Kim, H.L. Stormer, Phys. Rev. Lett. 98 (2007) 197403.
[8] Huynh Vinh Phuc, Nguyen Ngoc Hieu, Opt. Commun. 344 (2015) 12.
[9] Huynh Vinh Phuc, Le Dinh, Mater. Chem. Phys. 163 (2015) 116.
[10] E. Conwell, V.F. Weisskopp, Phys. Rev. 77 (1950) 388.
[11] P.M. Krstajic, P. Vasilopoulos, Phys. Rev. B 86 (2012) 115432.
[12] C.H. Yang, F.M. Peeters, W. Xu, Phys. Rev. B 82 (2010) 075401.
[13] C.M. Wang, X.L. Lei, Phys. Rev. B 87 (2013) 235403.
[14] Gianluca Giovannetti, Petr A. Khomyakov, Geert Brocks, Paul J. Kelly, Jeroen van den Brink, Phys. Rev. B 76 (2007) 073103.
[15] C.R. Dean, A.F. Young, I. Meric, C. Lee, L. Wang, S. Sorgenfrei, K. Watanabe, T. Taniguchi, P. Kim, K.L. Shepard, J. Hone, Nat. Nanotechnol. 5 (2010) 722.
[16] B. Sachs, T.O. Wehling, M.I. Katsnelson, A.I. Lichtenstein, Phys. Rev. B 84 (2011) 195414.
[17] S.Y. Zhou, G.-H. Gweon, A.V. Fedorov, P.N. First, W.A. de Heer, D.-H. Lee, F. Guinea, A.H. Castro Neto, A. Lanzara, Nature Mater. 6 (2007) 916.
[18] F. Varchon, R. Feng, J. Hass, X. Li, B. Ngoc Nguyen, C. Naud, P. Mallet, J.-Y. Veuillen, C. Berger, E.H. Conrad, L. Magaud, Phys. Rev. Lett. 99 (2007) 126805.
[19] A.H. Castro Neto, F. Guinea, N.M.R. Peres, K.S. Novoselov, A.K. and Geim, Rev. Modern Phys. 81 (2009) 109.
[20] Y. Zhang, Z. Jiang, J.P. Small, M.S. Purewal, Y.-W. Tan, M. Fazlollahi, J.D. Chudow, J.A. Jaszczak, H.L. Stormer, P. Kim, Phys. Rev. Lett. 96 (2006) 136806.
[21] C.M. Wang, X.L. Lei, Phys. Rev. B 92 (2015) 125303.
[22] V.A. Margulis, J. Exp. Theor. Phys. 99 (2004) 633.
[23] Guang S. He, Nonlinear Optics and Photonics, OUP Oxford, 2014.
[24] G.S. He, P.P. Markowicz, T.C. Lin, P.N. Prasad, Nature 415 (2002) 767.
[25] W. Denk, J.H. Strickler, W.W. Webb, Science 248 (1990) 73.
[26] B.D. Hoi, L.T.T. Phuong, T.C. Phong, Superlattices Microstruct. 100 (2016) 365.
[27] D.Q. Khoa, L.T.T. Phuong, B.D. Hoi, Superlattices Microstruct. 103 (2017) 252.
[28] Chuong V. Nguyen, Nguyen N. Hieu, Do Muoi, Carlos A. Duque, Elmustapha Feddi, Hieu V. Nguyen, Le T.T. Phuong, Bui D. Hoi, Huynh V. Phuc, J. Appl. Phys. 123 (2018) 034301.
[29] Yun Wu, Xuming Zou, Menglong Sun, Zhengyi Cao, Xinran Wang, Shuai Huo, Jianjun Zhou, Yang Yang, Xinxin Yu, Yuechan Kong, Guanghui Yu, Lei Liao, Tangsheng Chen, ACS Appl. Mater. Interfaces 8 (39) (2016) 25645.
[30] S.Y. Zhou, G.-H. Gweon, A.V. Fedorov, P.N. First, W.A. de Heer, D.-H. Lee, F. Guinea, A.H. Castro Neto, A. Lanzara, Nature Mater. 6 (2007) 770.
[31] J.H. Grönqvist, T. Stroucken, G. Berghäuser, S.W. Koch, 2011, arXiv:1107.5653.
[32] Hamin Park, Tae Keun Kim, Sung Woo Cho, Hong Seok Jang, Sang Ick Lee, Sung-Yool Choi, Sci. Rep. 7 (2017) 40091.
[33] B. Scharf, V. Perebeinos, J. Fabian, I. Zuti, Phys. Rev. B 88 (2013) 125429.
[34] C.J. Tabert, E.J. Nicol, Phys. Rev. B 88 (2013) 085434.
[35] C.V. Nguyen, N.N. Hieu, N.A. Poklonski, V.V. Ilyasov, L. Dinh, T.C. Phong, L.V. Tung, H.V. Phuc, Phys. Rev. B 96 (2017) 125411.